Hyeyoung Nam,[1] Deborah Jones,[1] Robert C. Cooksey,[1] Yan Gao,[2] Sandy Sink,[2] James Cox,[3] and Donald A. McClain[1,2,3]

Synergistic Inhibitory Effects of Hypoxia and Iron Deficiency on Hepatic Glucose Response in Mouse Liver

Hypoxia and iron both regulate metabolism through multiple mechanisms, including hypoxia-inducible transcription factors. The hypoxic effects on glucose disposal and glycolysis are well established, but less is known about the effects of hypoxia and iron deficiency on hepatic gluconeogenesis. We therefore assessed their effects on hepatic glucose production in mice. Weanling C57BL/6 male mice were fed an iron-deficient (4 ppm) or iron-adequate (35 ppm) diet for 14 weeks and were continued in normoxia or exposed to hypoxia (8% O_2) for the last 4 weeks of that period. Hypoxic mice became hypoglycemic and displayed impaired hepatic glucose production after a pyruvate challenge, an effect accentuated by an iron-deficient diet. Stabilization of hypoxia-inducible factors under hypoxia resulted in most glucose being converted into lactate and not oxidized. Hepatic pyruvate concentrations were lower in hypoxic mice. The decreased hepatic pyruvate levels were not caused by increased utilization but rather were contributed to by decreased metabolism from gluconeogenic amino acids. Pyruvate carboxylase, which catalyzes the first step of gluconeogenesis, was also downregulated by hypoxia with iron deficiency. Hypoxia, and more so hypoxia with iron deficiency, results in hypoglycemia due to decreased levels of hepatic pyruvate and decreased pyruvate utilization for gluconeogenesis. These data highlight the role of iron levels as an important determinant of glucose metabolism in hypoxia.

Iron and hypoxia both have significant effects on a wide range of metabolic processes (1,2), but their potential interactions in determining metabolism are poorly understood.

Hypoxia results in stabilization of hypoxia-inducible factors (HIFs), transcription factors that control a wide range of physiologic processes. HIF-1 and -2 form heterodimeric DNA binding complexes composed of α- and β-subunits (3). HIF-1α and HIF-2α are highly structurally homologous; however, the phenotypes of HIF-1α and HIF-2α knockout mice differ in the effects on transcriptional targets and their tissue distribution (4). Under normoxia, HIF-α subunits are hydroxylated at proline residues by prolyl hydroxylase (PHD) and then rapidly degraded by the ubiquitin-proteasome pathway. PHDs are 2-oxoglutarate–dependent dioxygenases that use O_2 as a substrate and iron as a cofactor. Thus, under hypoxia or iron deficiency, the catalytic activity of PHDs is inhibited, allowing HIF-α subunits to escape degradation and translocate to the nucleus, where they dimerize with β-subunits to activate transcription (5). Iron metabolism is tightly coregulated with oxygen homeostasis, and HIFs regulate genes involved in iron uptake and utilization.

Hypoxia is associated with multiple changes in metabolism and energy balance. Decreased weight and/or weight loss, for example, is seen in individuals living at high altitude (6) or in high-altitude sojourners. The mechanisms underlying these effects, however, are not completely understood. Decreased appetite and caloric intake frequently occur at altitude, and some but not all studies suggest a relation to increased levels of leptin, an HIF-1α–responsive gene (7,8). Living at high altitude is also associated with lower fasting blood glucose levels and improved glucose tolerance (9). Tibetans, for example, commonly live at altitudes of up to 5,000 m and have successfully adapted to high altitude (10). Tibetans are not only protected

METABOLISM

[1]Department of Internal Medicine, University of Utah, Salt Lake City, UT
[2]Department of Internal Medicine, Wake Forest School of Medicine, Winston-Salem, NC
[3]Department of Biochemistry, University of Utah, Salt Lake City, UT
Corresponding author: Donald A. McClain, dmcclain@wakehealth.edu.

from mountain sickness but also have a lower prevalence of diabetes and metabolic syndrome (11). The mechanisms related to changes in weight and improved glucose handling among individuals accustomed to higher altitude are incompletely understood, but the contribution of the HIF pathway is supported by observations in pathologic activation of hypoxia-sensing pathways at lower altitudes.

The disease Chuvash polycythemia (CP), for example, is characterized by mutation of the VHL protein and impaired degradation of HIF-1α and HIF-2α, even under normoxia. CP patients have lower blood glucose levels and glycosylated hemoglobin A_{1c} levels compared with wild-type subjects (12). Studies in mice with the cognate human mutation suggest the relative hypoglycemia in CP results from a combination of effects on hepatic gluconeogenesis and increased glucose disposal (12). CP is frequently treated by phlebotomy to manage HIF-induced polycythemia, but the effects of the resulting iron loss on the glucose phenotype are unknown. Approximately 7% of the world's population lives above 1,500 m altitude (13), and 2 billion people in the world suffer from iron deficiency (14). The interactions of hypoxia pathways with iron levels in affecting glucose metabolism are therefore highly clinically relevant but understudied.

To test the hypothesis that dietary iron deficiency and hypoxia interact to affect glucose homeostasis, weanling male mice were fed iron-deficient (FeD) or iron-adequate (FeA) diets and subsequently exposed to normoxia or hypoxia (8% O_2). Hypoxic mice became hypoglycemic due to the impairment of hepatic glucose production for multiple reasons, including decreased levels of pyruvate despite increased levels of gluconeogenic amino acids, decreased levels of pyruvate carboxylase (PC), and decreased expression of enzymes involved in processing gluconeogenic amino acids. These effects were exacerbated by iron deficiency, suggesting that tissue iron stores may be an important determinant of glucose metabolism in hypoxia.

RESEARCH DESIGN AND METHODS

Experimental Animals
Weanling C57BL/6 male mice (n = 4–5/group) were given free access to Harlan AIN-93G diets containing iron at 4 mg/kg (TD.10210) for an FeD diet or 35 mg/kg (TD.10211) for an FeA diet for 14 weeks (by weight 17.7% protein, 60.1% carbohydrate, and 7.2% fat; Harlan Teklad, Madison, WI). Weanling mice were fed the same diets for 10 weeks and then transferred into a hypoxia chamber and exposed to 8% O_2 for 4 weeks with continuation of the same diets. The experiment design is summarized in Fig. 1. Oxygen levels were regulated by a ProOx 110 oxygen controller (BioSpherix). The chamber was opened for ~10 min every 3 days for maintenance and refeeding. At the end of the studies, animals were anesthetized with isoflurane, and blood collection was performed by cardiac puncture. Animal protocols were approved by the University of Utah and Wake Forest University Institutional Animal Care and Use Committees.

Pyruvate and Alanine Tolerance Test
For the pyruvate or alanine tolerance test, mice were fasted for 16 h, followed by an intraperitoneal injection of sodium pyruvate or L-alanine (2 g/kg body weight). Tail blood was taken at specified times, and glucose levels were measured by glucometer (Bayer Contour).

Measurement of Blood Parameters and Hepatic Iron Concentrations
Hemoglobin was measured with a HemoCue201$^+$ analyzer (HemoCue). Plasma insulin levels were measured by ELISA (Crystal Chem Inc.), plasma lactate and alanine by kit (Sigma-Aldrich), and liver total iron (nonheme and heme) levels by inductively coupled plasma mass spectroscopy conducted by the diagnostic center at Michigan State University (15,16).

RNA Isolation and Quantitative RT-PCR
Total RNA was isolated using the RNeasy Mini Kit (Qiagen). cDNA synthesis and RT-PCR were described previously (16). Primer sequences are given in Supplementary Table 1.
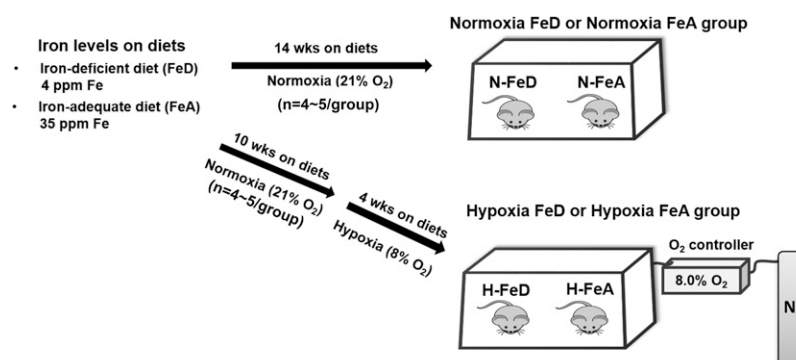
Figure 1—Schematic experimental design for normoxia and hypoxia animal studies. Weanling male mice were randomized in FeD and FeA diets (n = 4–5/group). The N-FeD and N-FeA mice were fed these diets for 14 weeks. For hypoxic treatment, weanling mice were fed the same diets for 10 weeks and then exposed to 8% O_2 for 4 weeks with continuation of the same diets. wks, weeks.

Immunoblotting Analysis

Liver samples were homogenized in ice-cold radioimmunoprecipitation assay buffer (Sigma-Aldrich) containing $1\times$ Complete Mini Protease Inhibitor Cocktail (Roche). Preparation of samples and Western blot analysis were described previously (16). Antibodies used included HIF-1α (Pierce), HIF-2α (Novus Bio), tubulin (Sigma-Aldrich), phosphorylated mammalian target of rapamycin (p-mTOR), mTOR, protein LC3 (LC3I), LC3I conjugated to phosphatidylethanolamine (LC3II), p62, and Atg3 (autophagy family 3) (Cell Signaling).

Determination of PC Activity

PC activity in liver mitochondria was measured as previously described (17) by incubating aliquots of crude mitochondria with reaction mixtures containing 4 mmol/L ^{14}C NaHCO$_3$ (PerkinElmer). Activities were expressed as picomoles of oxaloacetate formed per milligram of protein per min.

Hepatic Glucose Production Assay

HepG2 cells were transfected with 10 nmol/L human HIF-1α, HIF-2α, or negative control small interfering RNA (si)RNA (Qiagen) using lipofectamine RNAiMAX (Invitrogen). After 48 h, cells were exposed to normoxia or hypoxia (1% O_2 and 5% CO_2) at 37°C (Galaxy 48R CO_2 incubator; Eppendorf) in the presence or absence of 100 μmol/L desferrioxamine (DFO) for 24 h. Cells were incubated with phenol red–free, glucose-free DMEM (Invitrogen) containing 2 mmol/L pyruvate, 20 mmol/L lactate, and 10 μmol/L forskolin (Sigma-Aldrich). The medium was collected 3 h later, and glucose levels in the medium were measured by kit (Sigma-Aldrich).

Glucose Incorporation and Metabolomic Analyses

HepG2 cells were supplemented with fresh 25 mmol/L [U-$^{13}C_6$]glucose (Cambridge Isotope Laboratories). After 24 h, metabolites were extracted by adding cold 80% high-performance liquid chromatography–grade methanol, as described previously (18). Gas chromatography–mass spectrometry (GC-MS) analyses were conducted using an Agilent 6890N connected to a Waters GCT Premier detector equipped with a Zebron ZB-5MSi Guardian column and an HP7682 injector. The QaunLynx software program (Waters) was used to extract and integrate the target compounds. Samples were normalized to the internal standard D$_4$-succinate and protein concentrations. For in vivo studies, freeze-clamped liver tissue was homogenized in bead mill tubes containing cold 90% MeOH with internal standards (D$_4$-succinate). The sample was homogenized, placed at −20°C for 1 h to precipitate proteins, and centrifuged at 20,000g for 5 min at 4°C. The supernatant was collected, dried under vacuum, and subjected to GC-MS as described above.

Statistical Analysis

Results are expressed as means $\pm$ SE. The significance of variability was determined by two-way ANOVA and the Tukey multiple comparison post hoc test. Data were analyzed with GraphPad Prism software.

RESULTS

Hypoxic Mice Become Hypoglycemic

Mice were provided at weaning with a normal purified FeA diet (35 ppm) or the same purified FeD diet (4 ppm). Groups were separated 10 weeks later and were continued under normoxia or exposed to hypoxia (8% O_2) for a further 4 weeks. Mice were killed, and hemoglobin levels were 33% higher in hypoxic (H) mice fed the FeA diet (H-FeA) compared with normoxic (N) mice fed the same diet (N-FeA). Hypoxic mice fed the FeD (H-FeD) became anemic, as indicated by reduced hemoglobin relative to that of N-FeA and H-FeA mice (Fig. 2A). Total liver iron concentrations trended to be decreased in N-FeD mice compared with N-FeA mice. In H-FeD mice, liver total iron levels were three times lower than in N-FeA or H-FeD mice (Fig. 2B). After 12 h fasting, normoxic mice maintained blood glucose values in the 65–70 mg/dL range. Glucose levels were significantly decreased in hypoxia (Fig. 2C). Fasting glucose values of H-FeD mice were decreased by 31% compared with N-FeD and H-FeA by 46% compared with N-FeA. Insulin levels were increased by 70% in H-FeD mice and by 109% in H-FeA mice relative to N-FeA controls (Fig. 2D).

Significant decreases in body weight were observed in hypoxic mice after exposure to hypoxia (Supplementary Fig. 1). The levels of food intakes did not differ among the group for 10 weeks on the different iron diets (Supplementary Fig. 1C). The initial exposure of hypoxia caused a significant decrease in food intake in both H-FeD and H-FeA mice on day 3. During the subsequent 3 weeks, food intake recovered, and food intake for the final 3 weeks did not differ among the groups. This finding is consistent with results of other reports (19,20). Leptin levels were increased by iron deficiency but not significantly so by hypoxia (data not shown), indicating that leptin was not solely responsible for the changes in food intake. Mice were killed and body was composition was analyzed by dual photon absorptiometry. Lean mass did not differ among the groups, although hypoxic mice fed both diets exhibited decreased fat mass and bone mineral content (Supplementary Fig. 1D).

Hepatic Glucose Production Is Impaired in Hypoxic Mice but Not due to Decreased Gluconeogenic Gene Expression

To determine if the observed hypoglycemia was due to changes in endogenous glucose production, we performed pyruvate and alanine tolerance testing, wherein blood glucose excursions are measured after an intraperitoneal injection of either of those two gluconeogenic precursors in mice fasted overnight. Injection of pyruvate resulted in a rapid increase in blood glucose levels in normoxic mice (Fig. 3A). However, the H-FeA mice displayed impaired glucose production, and the H-FeD mice exhibited a further decrease (Fig. 3A and B). Similarly, blood glucose levels were increased in N-FeA mice after injection of L-alanine, whereas N-FeD mice had less glucose production
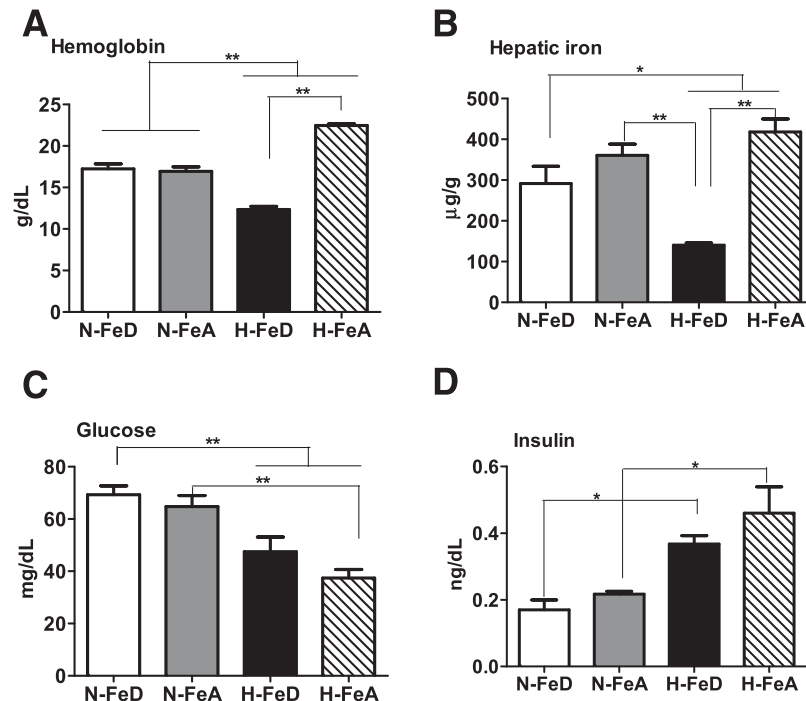
Figure 2—Hemoglobin, hepatic iron, blood glucose, and insulin levels in normoxic or hypoxic mice on the varied iron diets. *A*: Hemoglobin levels of N-FeD, N-FeA, H-FeD, and H-FeA mice. *B*: Hepatic iron (heme and nonheme) levels were determined by inductively coupled plasma mass spectroscopy and are reported as micrograms of Fe per gram of tissue dry weight. The levels of glucose (*C*) and plasma insulin (*D*) were analyzed after overnight fasting. Values are expressed as mean ± SE (*n* = 4–5 per group). *$P < 0.05$ and **$P < 0.01$ indicate the difference among the groups.

(Fig. 3*C*). H-FeA mice exhibited further impairment in their glucose response, and this was yet more accentuated in the H-FeD mice (Fig. 3*C* and *D*). We next determined if the impairment of glucose response was contributed by downregulation in the expression of genes for gluconeogenic enzymes. Despite increased insulin (Fig. 2*D*), mRNA expression of neither phosphoenolpyruvate carboxykinase (PEPCK) nor glucose-6-phosphatase (G6Pase) was changed in H-FeD mice (Fig. 3*E* and *F*).

H-FeD Mice Have Increased Plasma Levels of Gluconeogenic Substrates, and Glucose Is Preferentially Converted Into Lactate Rather Than Pyruvate

Levels of plasma lactate and alanine were measured to determine if hypoglycemia in hypoxic mice was due to diminished availability of those metabolites, the principal gluconeogenic precursors in the blood. Lactate and alanine, however, were increased by 161% and 74% in H-FeD relative to N-FeA mice (Fig. 4*A* and *B*). The increased levels of lactate in H-FeD mice may have been due to increased production in skeletal muscle, insofar as glucose oxidation rates were down (Supplementary Fig. 2*A*), and mRNA levels of lactate dehydrogenase A were increased (Supplementary Fig. 2*D*) in the H-FeD cohort. The increase in lactate was unlikely to be caused solely by hypoxia-driven lactate release from muscle because the mRNA levels of the hypoxia-responsive monocarboxylate

transporter 4 were not increased in the H-FeD cohort, although they were increased in the H-FeA group (Supplementary Fig. 2*C*). Normally, these gluconeogenic precursors are converted into pyruvate in the liver for gluconeogenesis, but decreased levels of hepatic pyruvate were observed in hypoxic mice; hepatic lactate did not differ among the groups (Fig. 4*C* and *D*). These results suggest that decreased utilization of pyruvate for gluconeogenesis may have been occurring in the liver, so we next investigated the metabolic fates of pyruvate in the liver under hypoxia with or without iron deficiency.

Under aerobic conditions, pyruvate can enter into the citric acid (TCA) cycle for oxidative metabolism, with entry into the TCA cycle being tightly controlled by the activities of pyruvate dehydrogenase (PDH) and its inhibitory kinase (PDK). The mRNA levels of PDK isoform 2 (PDK2), which inhibits PDH and thus mitochondrial oxidation of pyruvate, were significantly upregulated in the liver of hypoxic mice (Fig. 4*E*). We did not measure glucose oxidation in liver tissue but did verify that glucose oxidation was decreased in isolated soleus muscle from hypoxic mice, with a further decrease being observed in H-FeD mice (45% decrease in H-FeA mice and 64% decrease in H-FeD mice compared with N-FeA mice) (Supplementary Fig. 2*A* and *B*), indicating that chronic hypoxia impairs entry of pyruvate into the TCA cycle. Thus, the decrease in hepatic pyruvate levels is unlikely to be caused by increased utilization in the TCA cycle.
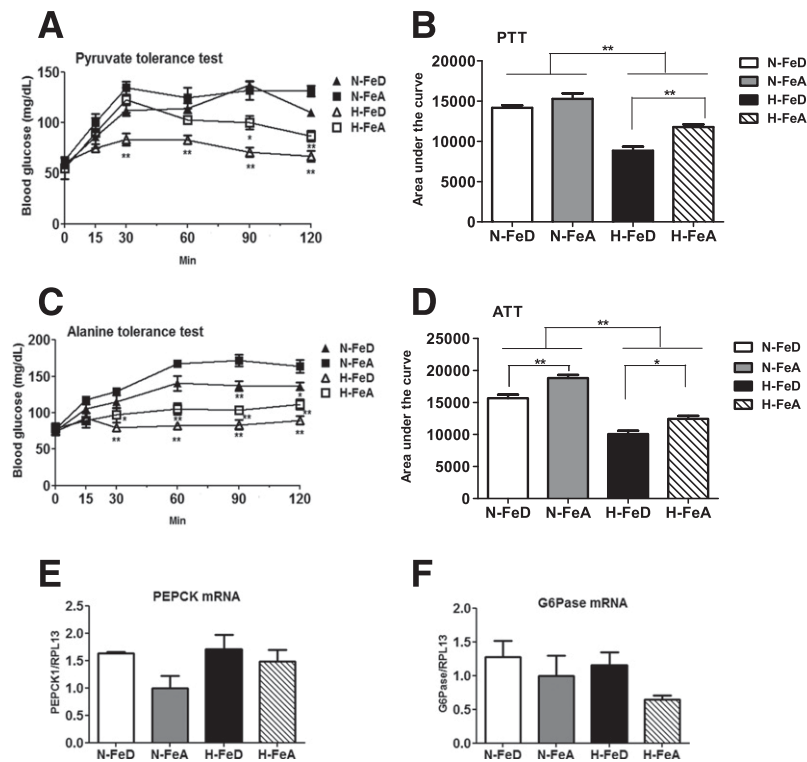
Figure 3—Hypoxia with iron deficiency impairs hepatic glucose production despite no change in the expression of gluconeogenic genes in mouse liver. For pyruvate (*A*) or alanine (*C*) tolerance testing, mice were fasted for 16 h, followed by an intraperitoneal injection of sodium pyruvate or L-alanine (2 g/kg body weight). *B* and *D*: The area under the glucose curve was calculated for the studies in *A* and *C*. Relative mRNA abundances of PEPCK (*E*) and G6Pase (*F*), normalized to levels of RPL13a, were determined by quantitative RT-PCR in mouse liver. Values are expressed as mean $\pm$ SE (*n* = 4–5 per group). ALT, alanine tolerance test; PTT, pyruvate tolerance test. *$P < 0.05$ and **$P < 0.01$ indicate the difference among the groups.
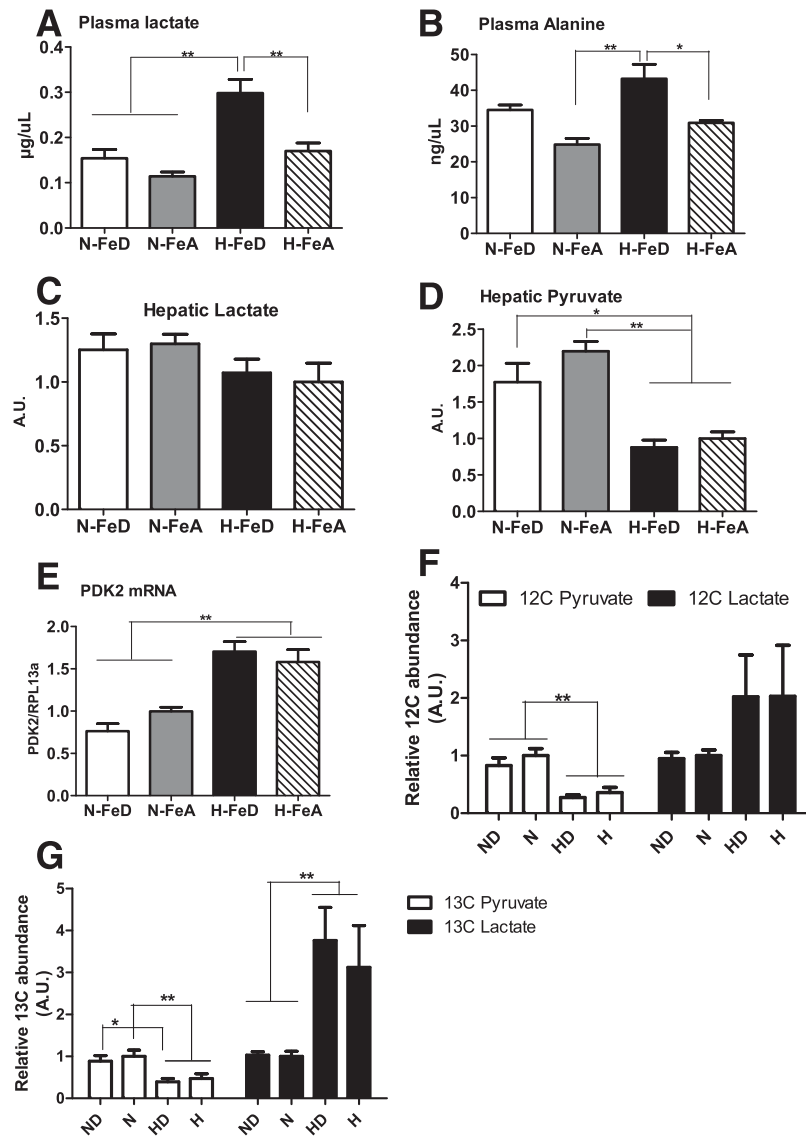
Pyruvate can also be converted into lactate in anaerobic glycolysis. We therefore examined the fate of uniformly labeled [U-^{13}C$_6$]glucose in HepG2 cells cultured in hypoxia (1% O$_2$), with or without iron depletion. Consistent with the results obtained in hypoxic mouse liver, total pyruvate levels were decreased and lactate levels were twofold higher under hypoxia (Fig. 4*F*). When the flux levels were assessed by incorporation of ^{13}C into lactate, the differences caused by hypoxia were even more pronounced (Fig. 4*G*). Treatment of cells with the iron chelator DFO further accentuated [^{13}C]lactate production. Thus, increased lactate production may be a factor in the observed decrease in pyruvate.

Hypoxia and Iron Deficiency Additively Stabilize HIFs, and HIF-1α Contributes to the Impairment of Hepatic Glucose Response Under Hypoxia and Iron Deficiency
Much of the shift in cellular metabolism to anaerobic processes under hypoxia is regulated by the HIF family of transcriptional factors that are stabilized under conditions of oxygen or iron insufficiency. Under normoxia, iron deficiency led to the upregulation of Hif1α (fourfold) and Hif2α (twofold) protein levels in liver compared with N-FeA mice (Fig. 5*A*). This effect was accentuated by the combination of iron deficiency and hypoxia (10-fold for Hif1α and 3-fold for Hif2α protein)

compared with N-FeA mice. The effects of hypoxia and iron deficiency on HIF expression were reflected in increased levels of mRNAs for Hif1α target genes: glycolytic enzymes (hexokinase 2 [HK2] and phosphofructokinase 1), sterol regulatory element–binding protein 1, and transferrin receptor 1 (TfR1) (Fig. 5*B*). HK2 and TfR1 mRNA levels were further upregulated by the combination of hypoxia and iron deficiency. TfR1 mRNA levels, which respond to iron status, were measured as a positive control for iron-dependent changes in these groups. As expected, TfR1 mRNA levels were upregulated in N-FeD or H-FeD mice relative to N-FeA or H-FeA mice.

To establish causality for the changes in HIF expression being responsible for changes in glucose production, HepG2 cells were treated with siRNA targeting human Hif1α or Hif2α, followed by hypoxia exposure. Treatment with Hif1α or Hif2α siRNA resulted in an 80% and 90% knockdown of each gene in hypoxia (Fig. 5*C*). We next examined glucose production by the HepG2 cells with knockdown of HIF expression by culturing in glucose-free medium containing the gluconeogenic precursors lactate and pyruvate and by measuring glucose accumulation in the media. In normoxia, hepatic glucose production in iron-depleted DFO-treated (ND) cells was slightly but not significantly higher than in control cells (Fig. 5*D*). However,
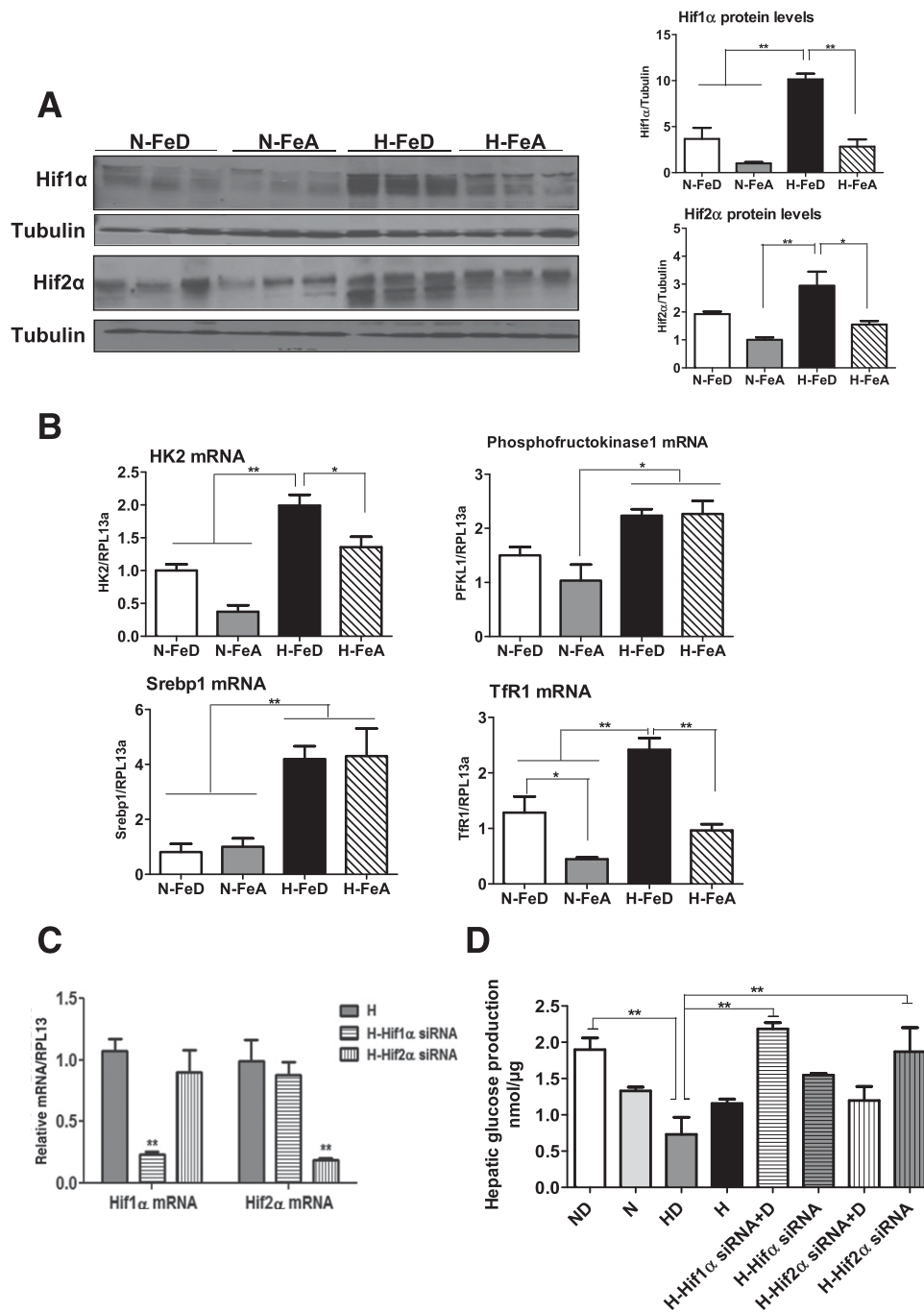
Figure 4—Hypoxia with iron deficiency upregulates plasma levels of gluconeogenic substrates, and glucose is preferentially converted into lactate rather than pyruvate. Levels of plasma lactate (*A*) and alanine (*B*) were analyzed in N-FeD, N-FeA, H-FeD, and H-FeA mice. The levels of hepatic lactate (*C*) and pyruvate (*D*) were measured by GC-MS in freeze-clamped liver tissue. *E*: Relative mRNA abundance of PDK2, normalized to levels of RPL13a, was determined by quantitative RT-PCR in mouse liver. Values are expressed as mean $\pm$ SE ($n = 4$–5 per group). *F*: HepG2 cells were incubated at normoxia in absence or presence of 100 μmol/L DFO. HepG2 cells were exposed to hypoxia (1% O_2 [H]) without or with iron depletion for 24 h. Relative abundances of [^{12}C]lactate and pyruvate were quantified with GC-MS. *G*: After 24 h incubation with uniformly labeled [^{13}C$_6$]glucose in HepG2 cells, the levels of [U-^{13}C]pyruvate and [U-^{13}C]lactate were measured using GC-MS. The bars represent the mean $\pm$ SE of three independent experiments performed in triplicate. A.U., arbitrary units. *$P < 0.05$ and **$P < 0.01$ indicate the difference among the groups.

under hypoxia (1% O_2), iron-depleted (HD) cells had reduced hepatic glucose production relative to that of ND cells. Knockdown of Hif1α under hypoxia resulted in recovery of the hepatic glucose response to levels seen in normoxia. Furthermore, the hepatic glucose response in Hif1α knockdown cells with DFO treatment was three times higher than in control HD cells. Although increased hepatic glucose response was seen in hypoxic cells treated with Hif2 siRNA, further increases in hepatic glucose response were not seen with incubation with DFO, suggesting that impaired hepatic glucose production under hypoxia with iron deficiency is mostly due to Hif1α induction.

PC Activity Is Downregulated in H-FeD Mice

Hepatic gluconeogenesis is initiated by PC, which is located in mitochondria and catalyzes the biotin-dependent carboxylation of pyruvate to oxaloacetate for initiating gluconeogenesis (Fig. 6*A*). Levels of PC mRNA in mouse liver were increased by iron deficiency under normoxia, but H-FeD significantly downregulated PC mRNA levels compared with N-FeD (Fig. 6*B*). Consistent with the mRNA expression, PC enzyme activity decreased by 80% under H-FeD, compared with the hypoxia control (Fig. 6*C*). Parallel results were observed in cultured cells, wherein hypoxic cells had 30% lower PC activity than normoxic

Figure 5—Hypoxia with iron deficiency leads to the stabilization of HIFs in mouse liver, and HIF-1α contributes to the impairment of hepatic glucose response. *A*: Immunoblot analysis of Hif1α and Hif2α in livers of normoxic or hypoxic mice. The blots were stripped and reprobed with tubulin as a lane loading control. The band intensities were quantified by the ImageJ program. *B*: The mRNA expression levels of the Hif1α target genes HK2, phosphofructokinase 1, sterol regulatory element–binding protein 1 (Srebp1), and TfR1 were analyzed by quantitative RT-PCR, and RPL13a was used as a normalizing gene. *C*: Human Hif1α, Hif2α, or negative control siRNA (10 nmol/L) was transfected in HepG2 cells, followed by exposure of 1% O_2 for 24 h (H-Hif1α and H-Hif2α siRNA). The transcript levels of Hif1α and Hif2α were analyzed by quantitative RT-PCR and normalized to human RPL13a. *D*: HepG2 cells were treated with Hif1α, Hif2α, or negative control siRNA and cultured in normoxia or under hypoxia (1% O_2 [H]) with or without 100 μmol/L of the iron chelator DFO for 24 h. After 24 h, the cells were incubated with hepatic glucose production buffer for 3 h. The glucose concentrations in medium were analyzed and normalized to protein levels. Bars represent the mean ± SE of three independent experiments performed in triplicate. *$P < 0.05$ and **$P < 0.01$ indicate the difference among the groups.
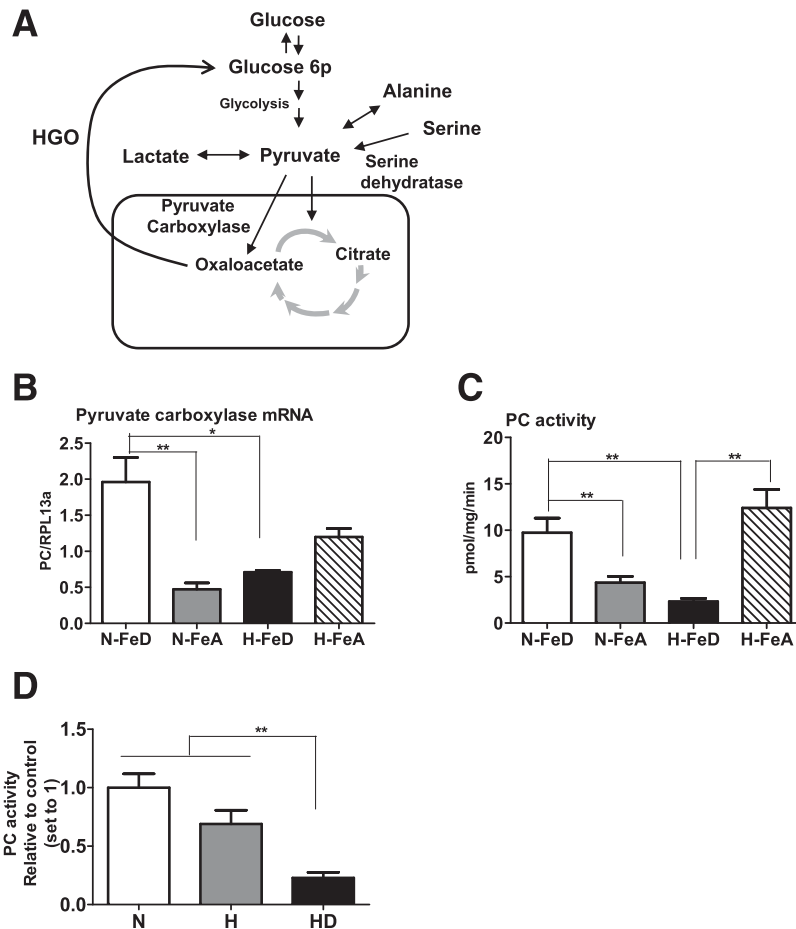
Figure 6—PC activity is significantly lower in hypoxia with iron deficiency. *A*: Simplified schematic diagram of the fates of pyruvate produced by glycolysis and hepatic gluconeogenesis. *B*: Relative transcript abundances of PC were analyzed by quantitative RT-PCR and normalized to RPL13a. *C*: The rates of PC activities were determined in freshly isolated crude mitochondria from mice livers. PC activity was assayed with a $[^{14}C]HCO_3^-$ fixation assay and expressed as picomoles of oxaloacetate formed per mg protein per min. *D*: HepG2 cells were exposed to 21% O_2 (N), 1% O_2 (H), or 1% O_2 with 100 μmol/L DFO (HD) for 24 h. Crude mitochondria were freshly isolated from these cells, followed by the incubation with PC activity reaction mixture. Bars represent the mean ± SE of three independent experiments performed in triplicate. HGO, hepatic glucose output. *$P < 0.05$ and **$P < 0.01$ indicate the difference among the groups.

cells, and the combined effect of H-FeD further diminished PC activity (~80% decrease in HD cells, Fig. 6*D*).

Levels of Serine Dehydratase mRNA Are Decreased and Levels of Gluconeogenic Amino Acids Are Increased in H-FeD Mice

We finally examined if the decreased pyruvate levels observed in H-FeD may also be contributed to by changes in the metabolism of the gluconeogenic amino acids that can be converted into pyruvate (Fig. 6*A*). Serine dehydratase, which converts serine into pyruvate, was ~60% lower in H-FeD mice compared with other groups (Fig. 7*A*). Therefore, pyruvate levels are lower in H-FeD as a result of multiple mechanisms, and the lack of pyruvate utilization for gluconeogenesis, in turn, results from lower levels of PC activity and of its substrate.

We next examined whether the levels of gluconeogenic amino acids that can be converted into pyruvate might also be responsible for decreased gluconeogenesis in H-FeD by quantitating their levels by GC-MS in freeze-clamped liver tissue. Serine, alanine, glycine, threonine, tryptophan, and cysteine were all increased in the livers of H-FeD mice (Fig. 7*B*), suggesting that decreased availability of these substrates was not contributing to decreased gluconeogenesis. To examine the reason for high levels of these amino acids, synthesis of gluconeogenic amino acids from glucose was measured by steady-state labeling of $[U-^{13}C_6]$glucose, followed by GC-MS analysis in HepG2 cells. The relative ^{13}C flux into amino acids from glucose carbon indicated that at least three amino acids—serine, glycine, and cysteine—exhibited decreased synthesis from glucose under hypoxia in the presence or absence of an iron chelator, suggesting that the increases in their total levels observed under hypoxia with
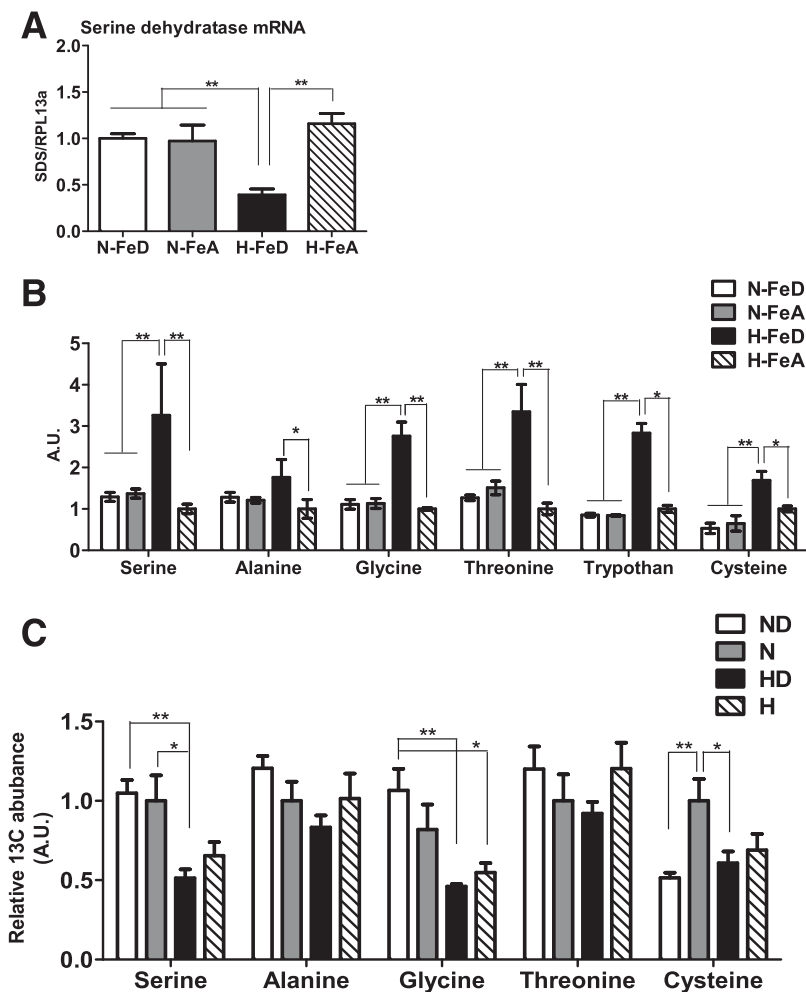
Figure 7—The levels of gluconeogenic amino acids are significantly upregulated by hypoxia and iron deficiency but not because of increased synthesis. *A*: Relative mRNA abundances of serine dehydratase, normalized to levels of RPL13a, were determined by quantitative RT-PCR *B*: Levels of gluconeogenic amino acids were analyzed by GC-MS with freeze-clamped liver tissues. *C*: HepG2 cells were supplemented with fresh 25 mmol/L [U-^{13}C$_6$]glucose. After labeling for 24 h, metabolites were extracted and analyzed by GC-MS. Bars represent the mean ± SE of three independent experiments performed in triplicate. A.U., arbitrary units; H, hypoxia (1% O$_2$). *$P < 0.05$ and **$P < 0.01$ indicate the difference among the groups.

iron deficiency were not due to their synthesis from glucose (Fig. 7*C*).

Decreased Anabolic and Increased Catabolic Signaling Induced by H-FeD in Mouse Liver

To examine the source of the increased amino acid levels in mouse liver exposed to H-FeD, we measured indices of activation of select anabolic and catabolic pathways. Most cells respond to nutritional deprivation by upregulating autophagy, a catabolic pathway, to maintain metabolic homeostasis and viability (21). A major intracellular hub for blocking autophagy-related signals is mTOR (22). The ratio of activated p-mTOR to total mTOR was significantly decreased in H-FeD mice compared with N-FeD mice (Fig. 8*A*). Furthermore, 4EBP1, a downstream target for mTOR signaling, is also regulated by both iron and hypoxia, as evidenced by changes in the p-4EBP1–to–4EBP1 ratio (Supplementary Fig. 3). A direct response

to autophagic signaling is the conjugation of LC3I with LC3II, experimentally determined by the LC3II-to-LC3I ratio. This ratio did not, however, change with hypoxia or iron deficiency (Fig. 8*B*). However, another autophagy marker, p62, whose levels are usually inversely corrected with autophagy, decreased 63% in H-FeD mice and 35% in H-FeA mice compared with N-FeA mice. Furthermore, Atg3, a protein required for autophagosome formation, was also upregulated in H-FeD and H-FeA compared with N-FeA mice. These data suggest that autophagy may play a role in the increased levels of gluconeogenic amino acids observed in hypoxia and iron deficiency.

DISCUSSION

Emerging evidence demonstrates that hypoxia and tissue iron stores both exert significant influences on glucose metabolism. Body iron stores are positively associated
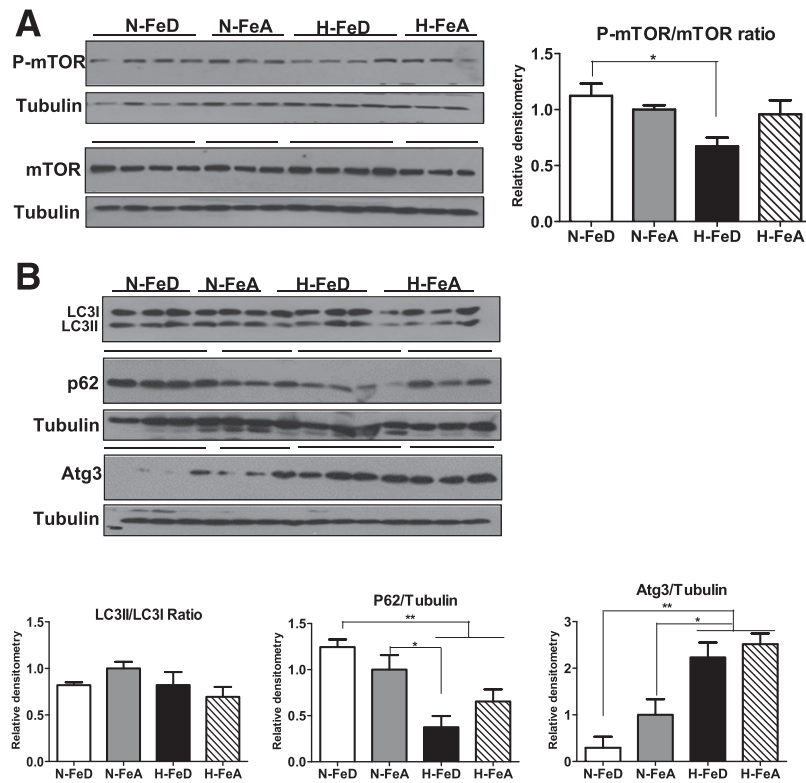
Figure 8—Decreased mTOR and increased autophagy signaling are observed in hypoxia and iron deficiency in mouse liver. *A*: Immunoblot analysis of p-mTOR and mTOR in livers of N-FeD, N-FeA, H-FeD, and H-FeA mice. *B*: Immunoblot analysis of LC3I and LC3II, p62, and Atg3 in mice livers of normoxic or hypoxic mice. The blots were stripped and reprobed with tubulin as a lane loading control. The band intensities were quantified by the ImageJ program. Values are expressed as mean ± SE (*n* = 4–5 per group). *P < 0.05 and **P < 0.01 indicate the difference among the groups.

with the development of glucose intolerance and type 2 diabetes (1). Conversely, phlebotomy improves glucose tolerance in prediabetes (23), and low levels of serum iron and its storage protein, ferritin, are associated with neonatal hypoglycemia (24). Because hypoxia and low iron can both signal additively through the hypoxia response pathway, we have investigated hepatic glucose metabolism in normoxic and hypoxic mice fed the FeD or FeA diets. We report here that hypoxic mice become hypoglycemic, largely due to the impairment of hepatic glucose production. These phenomena are accentuated in the H-FeD mice. The mechanisms for these effects include combined effects of hypoxia and iron deficiency on stabilization of HIFs, decreased hepatic levels of the gluconeogenic precursor pyruvate, and decreased levels of PC, the enzyme catalyzing the first step in gluconeogenesis. Decreased levels of hepatic pyruvate are caused by multiple mechanisms, including preferential conversion of glucose to lactate and decreased conversion of gluconeogenic precursor amino acids to hepatic pyruvate.

Consistent with our observations, individuals living at high altitude have been shown to have lower fasting glucose levels and better glucose tolerance compared with those who live at sea level (9,25). Higher insulin levels may contribute to the lower glycemia observed in

hypoxia in this study, but lower glucose levels of human highlanders are not adequately explained by insulin (26,27). More importantly, in the current studies we did not observe decreased expression of the rate-limiting enzymes in gluconeogenesis (PEPCK or G6Pase) that are responsive to high insulin. This observation supports the hypothesis that increased insulin levels do not wholly explain the observed hypoglycemia and do not contribute to the impairment of hepatic glucose production. The effects of hypoxia on insulin and insulin action are nevertheless interesting and deserve further study. Insulin levels would be expected to drop with the observed weight loss under hypoxia, for example, but in fact, insulin levels in the hypoxic group were higher than in the control group. Several studies have reported this paradoxical increase in insulin levels during weight loss under hypoxia and concluded that insulin levels are tightly related to duration and intensity of exposure to hypoxia (28–30). As a possible mechanism, hypoxia was previously demonstrated to increase insulin messenger stability (31). The parallel issue of insulin action during hypoxia has also received much attention.

Recently, researchers suggested that hepatic insulin signaling is sensitized by Hif2α stabilization through direct or indirect induction of insulin receptor substrate 2 (Irs2) and inhibition of vascular endothelial growth

factors (32). We compared hepatic Irs2 among the groups and did not observe any further induction of Irs protein levels in hypoxia (data not shown), supporting the conclusion that in our model, at least, the Irs mechanism is not involved. We examined the activation (phosphorylation) of the downstream mediator of insulin action, Akt, in liver, but the increased levels of insulin are not reflected in increased pAkt in the FeD mice (data not shown), suggesting insulin resistance upstream of that mediator. In the FeA mice, the increased insulin does cause increased pAkt (data not shown), but as we reported, this did not translate to repression of gluconeogenic gene expression, so in that case, there is an additional layer of insulin resistance distal to Akt. Further work will be needed to fully explicate these effects of hypoxia on insulin and insulin action, but because of the lack of any effects on gluconeogenic gene expression, we therefore sought other explanations for the changes in the fate and generation of hepatic pyruvate.

The mechanism for the decreased hepatic pyruvate levels seen with hypoxia and iron deficiency is likely multifactorial. Hypoxia and iron deficiency additively stabilize the protein levels of Hif1α and Hif2α that induce glycolysis through the upregulation of enzymes such as HK2 and phosphofructokinase 1 and inhibition of glucose oxidation by multiple mechanisms, including upregulation of PDK that inhibits PDH. The isoforms PDK2 and PDK4 are highly expressed in the liver (33), but only PDK2 is significantly upregulated by hypoxia. These results differ from previous reports that the mRNA for PDK4 but not PDK2 is induced by hypoxia (34). The differences may be accounted for by differences in the model systems and the degree and duration of hypoxia (9 h at 0.1% O_2) in the cited study. Regardless, the net effect of hypoxia and iron deficiency is to block the entry of glucose into the TCA cycle and preferentially convert it to lactate.

Other possible explanations for the decreased hepatic pyruvate levels include decreased metabolism from other sources. There are six gluconeogenic amino acids that can be converted into hepatic pyruvate. Levels of these amino acids were increased in the H-FeD mice, suggesting a possible block in their conversion to pyruvate. Consistent with this possibility, the mRNA level of serine dehydratase, which converts serine into pyruvate and whose activity is regulated at the level of transcription, is ~60% lower in hypoxia with iron deficiency (35). We noted no differences in other mRNAs that regulate conversion of gluconeogenic amino acids to hepatic pyruvate (e.g., alanine aminotransaminase 1 and cystathionase) but did not assess the enzyme activities associated with these transcripts.

Two important members of the HIF family are HIF-1α and HIF-2α. The metabolic effects of HIF-1α are largely related to effects on target genes involved in glucose uptake, glycolysis, and nonoxidative metabolism, although its effects vary according to tissue and degree of hypoxia

(36). HIF-2α, at least in the liver, primarily regulates lipid metabolism through decreased fatty acid oxidation and increased lipid storage (37). Transcription of the mRNAs for the rate-limiting enzymes in hepatic gluconeogenesis, PEPCK and G6Pase, is upregulated by HIF-1α (38). In mice exposed to hypoxia and/or iron deficiency, however, we did not observe changes in PEPCK or G6Pase expression that would explain the observed changes in hepatic glucose production. Hepatic gluconeogenesis is known to be coordinately modulated by multiple gluconeogenic enzymes (39), and several HIF-1 target genes are also regulated by hypoglycemia (40,41). One candidate for the effects observed in our studies is the mitochondrial enzyme PC, a known target of the hypoxia pathway that catalyzes the first committed step in gluconeogenesis (42). Indeed, we observed upregulation of PC transcripts in mice exposed to 8% O_2 for 3 days (data not shown), but PC transcripts were downregulated by long-term exposure of hypoxia in H-FeD compared with N-FeD mice. HIF target genes are known to be differentially expressed in acute compared with long-term hypoxia in mouse liver (43), and iron deficiency may induce additional pathways that contribute to the final integrated pathway of the hypoxia-acclimatized state. The importance of PC to our observed hypoglycemic phenotype is consistent with multiple observations. Deficiency of PC, for example, is a rare autosomal-recessive inborn error of metabolism that causes hypoglycemia and lactic acidosis (44). Hepatic PC protein levels are regulated by feeding/fasting and dysregulated in diabetes and are strongly correlated with glycemia in humans (45,46).

In investigating the mechanisms for decreased hepatic pyruvate levels, we observed that levels of gluconeogenic amino acids were upregulated by hypoxia with iron deficiency and that this was not due to increased de novo synthesis from glucose. This observation is consistent with others who demonstrated increased levels of intracellular amino acids in hypoxic cells (47). These amino acids likely derive from increased cell catabolism by autophagy. One pathway by which nutrient starvation triggers autophagy is through blocking of mTOR, a central regulator of cell growth and metabolic activity (22). We demonstrated decreased levels of mTOR signaling in hypoxia with iron deficiency. The ratio of LC3II to LC3I, one indicator of autophagic activity, did not differ among these groups. The conversion of LC3I to LC3II is catalyzed by autophagy-initiation protein Atg3, which was increased in hypoxic mice compared with normoxic mice. The fact that the LC3II-to-LC3I ratio was not, however, increased may reflect its faster degradation under hypoxia (48) and the known fact that decreased mTOR also decreases levels of LC3II (49). Consistent with the possibility that the ratio of LC3II to LC3I may not accurately reflect overall rates of autophagy in our model, p62 was significantly decreased in H-FeA mice relative to N-FeA mice and more so in H-FeD mice. The p62 protein preferentially interacts with LC3 to be degraded by autophagolysosomes (50); thus, the total

cellular expression levels of p62 are usually inversely correlated with autophagy activity.

In sum, we have presented evidence that hepatic glucose production is impaired in hypoxic mice and is further diminished in iron deficiency due to multiple mechanisms. Hypoxic mice demonstrate decreased levels of hepatic pyruvate despite increased levels of gluconeogenic amino acids, likely the result of activation of autophagy. PC, which catalyzes the first step for gluconeogenesis, is downregulated by hypoxia and iron deficiency. These data highlight the role of iron levels as an important determinant of glucose metabolism in hypoxia. These data also support the need for further studies on the effect of iron levels on other hypoxic conditions such as cancer or neonatal hypoglycemia.

References

1. Simcox JA, McClain DA. Iron and diabetes risk. Cell Metab 2013;17:329–341
2. Semenza GL. Oxygen sensing, hypoxia-inducible factors, and disease pathophysiology. Annu Rev Pathol 2014;9:47–71
3. Chachami G, Paraskeva E, Georgatsou E, Bonanou S, Simos G. Bacterially produced human HIF-1alpha is competent for heterodimerization and specific DNA-binding. Biochem Biophys Res Commun 2005;331:464–470
4. Loboda A, Jozkowicz A, Dulak J. HIF-1 and HIF-2 transcription factors–similar but not identical. Mol Cells 2010;29:435–442
5. Sutter CH, Laughner E, Semenza GL. Hypoxia-inducible factor 1alpha protein expression is controlled by oxygen-regulated ubiquitination that is disrupted by deletions and missense mutations. Proc Natl Acad Sci U S A 2000;97:4748–4753
6. Sherpa LY, Deji, Stigum H, Chongsuvivatwong V, Thelle DS, Bjertness E. Obesity in Tibetans aged 30-70 living at different altitudes under the north and south faces of Mt. Everest. Int J Environ Res Public Health 2010;7:1670–1680
7. Woolcott OO, Castillo OA, Torres J, Damas L, Florentini E. Serum leptin levels in dwellers from high altitude lands. High Alt Med Biol 2002;3:245–246
8. Tschöp M, Strasburger CJ, Hartmann G, Biollaz J, Bärtsch P. Raised leptin concentrations at high altitude associated with loss of appetite. Lancet 1998;352:1119–1120
9. Woolcott OO, Ader M, Bergman RN. Glucose homeostasis during short-term and prolonged exposure to high altitudes. Endocr Rev 2015;36:149–173
10. Beall CM, Cavalleri GL, Deng L, et al. Natural selection on EPAS1 (HIF2alpha) associated with low hemoglobin concentration in Tibetan highlanders. Proc Natl Acad Sci U S A 2010;107:11459–11464
11. Matsubayashi K, Kimura Y, Sakamoto R, et al. Comprehensive geriatric assessment of elderly highlanders in Qinghai, China I: activities of daily living, quality of life and metabolic syndrome. Geriatr Gerontol Int 2009;9:333–341
12. McClain DA, Abuelgasim KA, Nouraie M, et al. Decreased serum glucose and glycosylated hemoglobin levels in patients with Chuvash polycythemia: a role for HIF in glucose metabolism. J Mol Med (Berl) 2013;91:59–67
13. Cohen JE, Small C. Hypsographic demography: the distribution of human population by altitude. Proc Natl Acad Sci U S A 1998;95:14009–14014
14. Stoltzfus R. Defining iron-deficiency anemia in public health terms: a time for reflection. J Nutr 2001;131(2S-2):565S–567S
15. Nam H, Knutson MD. Effect of dietary iron deficiency and overload on the expression of ZIP metal-ion transporters in rat liver. Biometals 2012;25:115–124
16. Nam H, Wang CY, Zhang L, et al. ZIP14 and DMT1 in the liver, pancreas, and heart are differentially regulated by iron deficiency and overload: implications for tissue iron uptake in iron-related disorders. Haematologica 2013;98:1049–1057
17. Suormala T, Wick H, Bonjour JP, Baumgartner ER. Rapid differential diagnosis of carboxylase deficiencies and evaluation for biotin-responsiveness in a single blood sample. Clin Chim Acta 1985;145:151–162
18. Ye J, Mancuso A, Tong X, et al. Pyruvate kinase M2 promotes de novo serine synthesis to sustain mTORC1 activity and cell proliferation. Proc Natl Acad Sci U S A 2012;109:6904–6909
19. van den Borst B, Schols AM, de Theije C, et al. Characterization of the inflammatory and metabolic profile of adipose tissue in a mouse model of chronic hypoxia. J Appl Physiol (1985) 2013;114:1619–1628
20. de Theije CC, Langen RC, Lamers WH, Schols AM, Köhler SE. Distinct responses of protein turnover regulatory pathways in hypoxia- and semistarvation-induced muscle atrophy. Am J Physiol Lung Cell Mol Physiol 2013;305:L82–L91
21. Mizushima N, Klionsky DJ. Protein turnover via autophagy: implications for metabolism. Annu Rev Nutr 2007;27:19–40
22. Blommaart EF, Luiken JJ, Blommaart PJ, van Woerkom GM, Meijer AJ. Phosphorylation of ribosomal protein S6 is inhibitory for autophagy in isolated rat hepatocytes. J Biol Chem 1995;270:2320–2326
23. Gabrielsen JS, Gao Y, Simcox JA, et al. Adipocyte iron regulates adiponectin and insulin sensitivity. J Clin Invest 2012;122:3529–3540
24. Amarnath UM, Ophoven JJ, Mills MM, Murphy EL, Georgieff MK. The relationship between decreased iron stores, serum iron and neonatal hypoglycemia in large-for-date newborn infants. Acta Paediatr Scand 1989;78:538–543
25. Srivastava KK, Kumria MM, Grover SK, Sridharan K, Malhotra MS. Glucose tolerance of lowlanders during prolonged stay at high altitude and among high altitude natives. Aviat Space Environ Med 1975;46:144–146
26. Lindgärde F, Ercilla MB, Correa LR, Ahrén B. Body adiposity, insulin, and leptin in subgroups of Peruvian Amerindians. High Alt Med Biol 2004;5:27–31
27. Castillo O, Woolcott OO, Gonzales E, et al. Residents at high altitude show a lower glucose profile than sea-level residents throughout 12-hour blood continuous monitoring. High Alt Med Biol 2007;8:307–311
28. Young PM, Rose MS, Sutton JR, Green HJ, Cymerman A, Houston CS. Operation Everest II: plasma lipid and hormonal responses during a simulated ascent of Mt. Everest. J Appl Physiol (1985) 1989;66:1430–1435
29. Chaiban JT, Bitar FF, Azar ST. Effect of chronic hypoxia on leptin, insulin, adiponectin, and ghrelin. Metabolism 2008;57:1019–1022
30. Siervo M, Riley HL, Fernandez BO, et al.; Caudwell Xtreme Everest Research Group. Effects of prolonged exposure to hypobaric hypoxia on oxidative stress, inflammation and gluco-insular regulation: the not-so-sweet price for good regulation. PLoS One 2014;9:e94915
31. Tillmar L, Welsh N. Hypoxia may increase rat insulin mRNA levels by promoting binding of the polypyrimidine tract-binding protein (PTB) to the pyrimidine-rich insulin mRNA 3′-untranslated region. Mol Med 2002;8:263–272
32. Wei K, Piecewicz SM, McGinnis LM, et al. A liver Hif-2α-Irs2 pathway sensitizes hepatic insulin signaling and is modulated by Vegf inhibition. Nat Med 2013;19:1331–1337

33. Gudi R, Bowker-Kinley MM, Kedishvili NY, Zhao Y, Popov KM. Diversity of the pyruvate dehydrogenase kinase gene family in humans. J Biol Chem 1995; 270:28989–28994

34. Lee JH, Kim EJ, Kim DK, et al. Hypoxia induces PDK4 gene expression through induction of the orphan nuclear receptor ERRγ. PLoS One 2012;7: e46324

35. Su Y, Kanamoto R, Miller DA, Ogawa H, Pitot HC. Regulation of the expression of the serine dehydratase gene in the kidney and liver of the rat. Biochem Biophys Res Commun 1990;170:892–899

36. Williams KJ, Telfer BA, Airley RE, et al. A protective role for HIF-1 in response to redox manipulation and glucose deprivation: implications for tumorigenesis. Oncogene 2002;21:282–290

37. Rankin EB, Rha J, Selak MA, et al. Hypoxia-inducible factor 2 regulates hepatic lipid metabolism. Mol Cell Biol 2009;29:4527–4538

38. Choi JH, Park MJ, Kim KW, et al. Molecular mechanism of hypoxia-mediated hepatic gluconeogenesis by transcriptional regulation. FEBS Lett 2005;579:2795–2801

39. Burgess SC, He T, Yan Z, et al. Cytosolic phosphoenolpyruvate carboxykinase does not solely control the rate of hepatic gluconeogenesis in the intact mouse liver. Cell Metab 2007;5:313–320

40. Maltepe E, Schmidt JV, Baunoch D, Bradfield CA, Simon MC. Abnormal angiogenesis and responses to glucose and oxygen deprivation in mice lacking the protein ARNT. Nature 1997;386:403–407

41. Stein I, Neeman M, Shweiki D, Itin A, Keshet E. Stabilization of vascular endothelial growth factor mRNA by hypoxia and hypoglycemia and coregulation with other ischemia-induced genes. Mol Cell Biol 1995;15: 5363–5368

42. Arreola A, Cowey CL, Coloff JL, Rathmell JC, Rathmell WK. HIF1α and HIF2α exert distinct nutrient preferences in renal cells. PLoS One 2014;9:e98705

43. Baze MM, Schlauch K, Hayes JP. Gene expression of the liver in response to chronic hypoxia. Physiol Genomics 2010;41:275–288

44. Marin-Valencia I, Roe CR, Pascual JM. Pyruvate carboxylase deficiency: mechanisms, mimics and anaplerosis. Mol Genet Metab 2010;101:9–17

45. Kumashiro N, Beddow SA, Vatner DF, et al. Targeting pyruvate carboxylase reduces gluconeogenesis and adiposity and improves insulin resistance. Diabetes 2013;62:2183–2194

46. Hagopian K, Ramsey JJ, Weindruch R. Krebs cycle enzymes from livers of old mice are differentially regulated by caloric restriction. Exp Gerontol 2004;39: 1145–1154

47. Frezza C, Zheng L, Tennant DA, et al. Metabolic profiling of hypoxic cells revealed a catabolic signature required for cell survival. PLoS One 2011;6: e24411

48. Chen JL, Lin HH, Kim KJ, Lin A, Forman HJ, Ann DK. Novel roles for protein kinase Cdelta-dependent signaling pathways in acute hypoxic stress-induced autophagy. J Biol Chem 2008;283:34432–34444

49. Spilman P, Podlutskaya N, Hart MJ, et al. Inhibition of mTOR by rapamycin abolishes cognitive deficits and reduces amyloid-beta levels in a mouse model of Alzheimer's disease. PLoS One 2010;5:e9979

50. Bjørkøy G, Lamark T, Brech A, et al. p62/SQSTM1 forms protein aggregates degraded by autophagy and has a protective effect on huntingtin-induced cell death. J Cell Biol 2005;171:603–614